ESTIMATION OF COLUMN BASE FLEXIBILITY IN INSTRUMENTED BUILDINGS

Amit Kanvinde[1], Tomasz Falborski[2], Ahmad Hassan[1]

[1]Department of Civil and Environmental Engineering, University of California, Davis
[2]Faculty of Civil and Environmental Engineering, Gdansk University of Technology, Poland

Abstract

The rotational fixity of column base connections in Steel Moment Resisting Frames (SMRFs) strongly influences their seismic response. However, approaches for estimating base fixity have been validated only against laboratory test data. In the present study these approaches are examined based on strong motion recordings from two instrumented SMRF buildings in California. Three-dimensional simulation models are constructed for these buildings, including the gravity framing and nonstructural stiffness. For each building, the base fixities are parametrically varied. These include pinned and fixed bases, as well as intermediate fixities determined from previously developed models that are appropriate to simulate the specific types of base connections used in the buildings. The simulated response of these buildings is compared to strong motion recordings to inform optimal approaches for simulating column bases.

Introduction

Steel Moment Resisting Frames (SMRFs) are popular lateral load resisting systems in seismically active regions, due to their ductility and the architectural versatility offered by unbraced bays. Consequently, research studies pertaining to SMRFs are very extensive – addressing member, connection, as well as system response. These studies have resulted in well-established design procedures for SMRFs, including for overall system design and member selection (AISC 341-16 [1]), beam-to-column connections (AISC 358-16 [2]), and column base connections (AISC *Design Guide One* – Fisher and Kloiber [3]). Despite these advances, one area (in the context of SMRFs) where the guidance is relatively less developed is the simulation of column base connections. This is because research on column base connections has lagged other SMRF connections (e.g., beam-column connections), such that the focus in the context of base connections has been on developing strength models (AISC *Design Guide One* – Fisher and Kloiber [3]) rather than stiffness or load-deformation response. The lack of research has been further fueled by the presumption that base connections respond either as fixed (if capacity designed to be stronger than the attached column) or as pinned (if designed otherwise). Following this presumption, base connections are simulated as either fixed or pinned in current design and performance assessment practice (Zareian and Kanvinde [4]). Recent research has shown this practice to be highly problematic for two reasons. First, experiments on various types of column base connections (shown in Figures 1a-c) ranging from exposed base plate connections (Gomez et al. [5]), slab-overtopped base plate connections (Barnwell [6]) and embedded base connections (Grilli et al. [7]) indicate that base connections exhibit partial fixity, which contravenes both the fixed and pinned assumptions. Second, the erroneous characterization of fixity (as either fixed or pinned) has significant implications for structural

response. For both these reasons, structural response is sensitive to estimates of base fixity, underscoring the need for its accurate characterization. Motivated by this, base fixity models have been proposed for various base connection details, including for exposed (Grilli et al. [7]), slab-overtopped (Tryon [8]), and embedded (Torres-Rodas [9]). Each of these models has been developed using (and validated against) a limited set of laboratory test data, typically associated with the research group that developed the models. Consequently, results from each model provide excellent agreement with laboratory data it is developed from (and moderately good agreement against other sets of data – see Torres-Rodas [9]). However, applying these models with confidence to simulate the rotational fixity of as-built field details is challenging for the following reasons: (1) the laboratory specimens investigate only a limited set of configuration details, i.e., anchor rod configurations, base plate shape and aspect ratio, surrounding reinforcement, such that extrapolation of the models to field details that are different has not been verified, (2) all laboratory specimens are loaded laterally under a constant axial load, whereas in the field, the axial load varies due to seismic motions – this is an important effect because axial load has a strong effect on the fixity of exposed base plate connections – Kanvinde et al. [10], (3) in practice, base connections are loaded under biaxial bending, whereas none of the models or tests have interrogated the effect of biaxial bending on rotational fixity, and (4) the laboratory specimens are anchored to a strong floor, such that the effect of soil deformations is not reflected in the test data.

Against this backdrop, this paper seeks to inform best practices for simulation of column base fixity in SMRFs using recorded time history data from two buildings instrumented as part of the California Strong Motion Instrumentation Program (Naeim et al. [11]). Sophisticated 3-dimensional frame models of these buildings are constructed, and various options (including the previously published models introduced above) for simulating column bases are evaluated by comparing the simulated response of these buildings to the recorded response under the recorded seismic excitations. To maximize confidence in the findings, the paper relies on objective error measures to compare the recordings with simulations, and highly detailed structural simulations including a process to independently evaluate the stiffness of nonstructural components.

Types of Column Base Connections and Flexibility Models

Referring to Figure 1 shown below, SMRF column base connections in seismically active regions of the US take numerous forms, depending on the loading, soil type, system design and architectural considerations, and local economies. Broadly, these may be categorized into exposed base plate connections, or embedded connections, with detailing variations (e.g., placement of anchor rods) within each form. The following subsections describe these connections, outlining the physical mechanisms by which they deform and resist loads, along with the models proposed to estimate their flexibility.
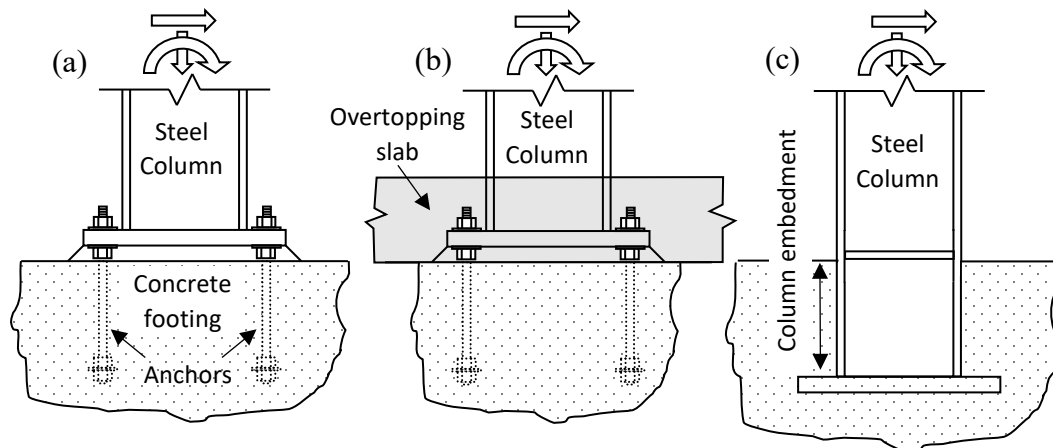
Figure 1. Common types of column base connections: (a) exposed base plate, (b) slab-overtopped exposed connections (c) embedded column base.

Exposed Base Plate Connections

Figure 1a shown previously schematically illustrates an exposed base plate connection in which the column is welded to a base plate, which is anchored to a footing using anchor rods, or post installed anchors (Gomez et al. [5]). The connection resists applied axial forces and moments through a combination of upward bearing on the compressive side of the connection and tensile forces in the anchor rods. In modern construction, usually a minimum of four anchor rods (near the corners of the connection) are provided to maintain erection stability as per OSHA [12]; these provide some degree of fixity even if the connection is not designed to carry significant moment. Additional anchor rods are often provided for supplemental strength. The connection itself is designed for the limit states of flexural yielding of the base plate, bearing failure in the footing, or anchor rode failure – by yielding, pullout or breakout (Steel Design Guide One [3]). Kanvinde et al. [10] presented a model to estimate the rotational flexibility of laboratory specimens with good accuracy (average test-predicted ratio $k_{base}^{test}/k_{base}^{model} = 0.89$). Subsequent research by Trautner [13] corroborates the validity of this model for other laboratory test data. Exposed base plate type connections are preferred for low- to mid-rise (less than 3-4 stories) SMRFs because it is economically unfeasible to transfer larger base moments through anchor rods; in such cases embedded base connections are typically specified.

Sometimes, exposed base connections are overtopped with a slab on grade (see Figure 1b); this is often the case in residential or commercial (as opposed to industrial) construction. The slab-on-grade is usually not considered in design, assuming that the connections respond in a manner similar to exposed base plate connections. However, studies by Barnwell [6] indicate that although the primary mechanism of load resistance is similar to the exposed base plate connections, the slab on grade (which is typically in the range of 150-200mm) increases the rotational fixity and provides additional strength as well. Tryon [8] proposed a model to estimate the rotational fixity of slab-overtopped connections. This model this model does not incorporate the effect of axial load since none of the laboratory specimens used for validation featured axial load.

Embedded Base Plate Connections

In contrast to slab-overtopped exposed base plate connections (Figure 1b) where in the embedment due to the slab is incidental, columns are often embedded in the footing by design (Figure 1c), to provide resistance through concrete bearing when exposed base plate connections with anchor rods become economically unfeasible. These connections are typically specified in mid- to high-rise buildings in which the moment demands are high. Referring to Figure 1c which shows such a connection, the load is resisted through a combination of horizontal bearing of the footing against the column flange, and vertical bearing against the embedded base plate. These mechanisms (identified by Grilli et al. [7] based on full-scale experiments) are the basis for a fixity model proposed by Torres-Rodas et al. [9] Although this model is able to characterize the stiffness of the experimental specimens with good accuracy (average test-predicted ratio $k_{base}^{test}/k_{base}^{model}$ =1.15), the experimental data set itself is relatively small (5 tests) and represents only one type of detail – similar to the one shown in Figure 1c. Variants of this configuration (for example using anchor rods in the embedded plates, or welded reinforcement attached to the column) are also prevalent. No test data exists for these, and consequently the efficacy of fixity models (Torres-Rodas et. al. [9]) is unknown as well.

Finally, none of these models (for any type of base connections) explicitly address the rotation of the footing itself, considering this to be a geotechnical/soil-structure interaction issue. This is because various footing designs (e.g., pedestal, raft, pile-cap) and soil types may be present along with features such as grade beams that connect the footings. Zareian and Kanvinde [4] proposed some recommendations for addressing these situations. Collectively, these models represent the state of the art for estimating base fixity in SMRFs. As described in a subsequent section, these models are used within frame models to examine their efficacy in reproducing recorded building motions.

Table 1. Building and CSMIP data characteristics.

Bldg	Location (all in CA)	CSMIP station	Stories	Square footage	Period (NS, EW, Estimate)	Base and foundation type	Sensors	Number of records and intensities $(S_a(T_1)/S_a^{DBE})$
1	Richmond	58506	3	37500 ft^2	0.60s, 0.76s, 0.59s	Exposed base plates with overtopping slabs concrete pile caps and grade beams	12	8 (0.162; 0.033; 0.017; 0.011; 0.008; 0.006; 0.005; 0.005)
2	Burbank	24370	6	86500 ft^2	1.29s, 1.33s, 0.96s	Embedded column bases connected to concrete pile caps and grade beams	13	7 (0.109; 0.085; 0.034; 0.011; 0.011; 0.003; 0.002)

Characteristics of Instrumented Buildings and Motions

Two SMRF buildings instrumented as part of the CSMIP were selected for analysis in this study. Table 1 shown above summarizes key characteristics of these buildings as well as the base connections used in these frames. Figures 2a-b illustrate these frames – each row of tiles within the figure represents one building (as indicated in the figure), whereas the columns show the photographs and structural models (first column), the moment frames (second column), and the gravity frames and the nonstructural components represented as braces (third column). Table 1 also indicates the normalized value of the geometric mean spectral acceleration for each of the records used in this study $S_a^{GM}/S_a^{10/50}$. This spectral acceleration is normalized by the design spectral acceleration (corresponding to a 10% probability of exceedance in 50 years) to provide a

sense of the intensity of the ground motions relative to building strength/design characteristics. Referring to these values, the intensity of ground motions is well below the design level, suggesting that that inelastic response is highly unlikely; this is later verified through the time history simulations. In each of the buildings, multiple accelerometers (oriented in orthogonal directions) are located on most story levels as well as at the ground level, enabling monitoring of effects such as torsion or unsymmetric response. In addition to the accelerograms recovered from these sensors, the CSMIP database also includes baseline corrected displacement time histories. The next section describes the frame models constructed to simulate these buildings.
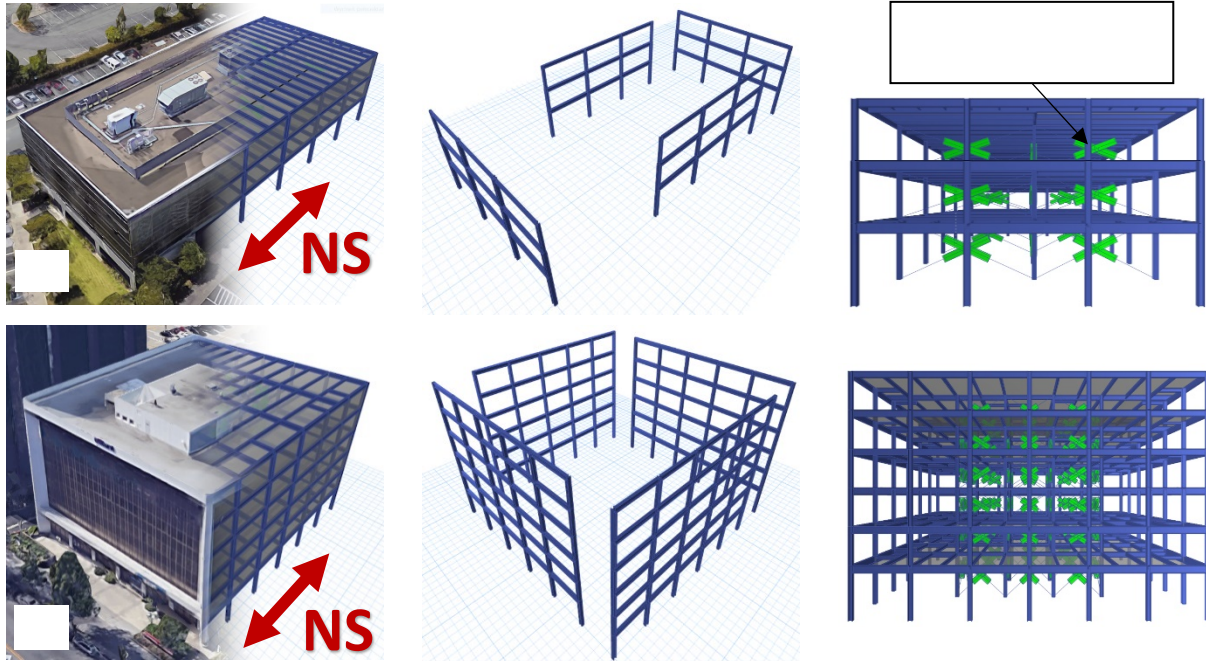
Figure 2. Selected buildings: (a) Building 1, (b) Building 2. Photograph and ETABS models (left column), Steel Moment Frames (middle column), and nonstructural bracing locations (right column).

Building Simulation Models

The main objective of the building simulations is to inform modeling practice for the column base connections, by varying column base fixity and examining the agreement between simulated and recorded response. To this end, it is especially important to minimize inaccuracies in the simulated frame/building response simulated by the building model such that the effect of base fixity may be evaluated with greater confidence. The building simulations are based on building drawings obtained from CSMIP; these drawings contain information regarding structural as well as nonstructural components, foundations, as well as connection details, including column base connections.

General Modeling Assumptions and Considerations

Three dimensional simulation models were constructed for all buildings using the software program ETABS [14]. In addition to the moment frames, the models included the

gravity frames, nonstructural components (i.e., partition and exterior walls) as well as diaphragms.

- All frames were simulated using 3-d elastic beam-column elements. The absence of inelastic response in all simulations was confirmed by performing post facto yielding checks in all members.
- Although inelastic response was not simulated, geometric nonlinearity was simulated to appropriately reflect P-Δ effects (due to the leaning effect of gravity frames) and the associated period elongation.
- Diaphragms were simulated as semirigid, accounting for the actual properties of the diaphragm including the steel decking and concrete.
- In the moment frames (indicated in Figure 2, second column), the beam-column connections were simulated as rigid, whereas in the gravity frames (Figure 2, third column), the beam-column connections were simulated as pinned; in both cases the columns were simulated as continuous through the height of the building.
- Finite joint size was modeled, along with panel zone flexibility.
- Seismic masses were assigned at each story level based on estimated dead loads as determined from the structural and nonstructural building drawings, as well as descriptions of finishes, as well as attached equipment and other masses that would contribute to seismic response. Over each story, the mass was uniformly distributed over the area of the diaphragm.
- The applied gravity loads reflect best estimates of both the dead and live loads. The total gravity loads are pertinent for accurate simulation of: (1) the leaning column or P-Δ effects, and (2) simulation of column base flexibility, especially for Building #1 with exposed column base plates whose fixity is sensitive to axial forces.
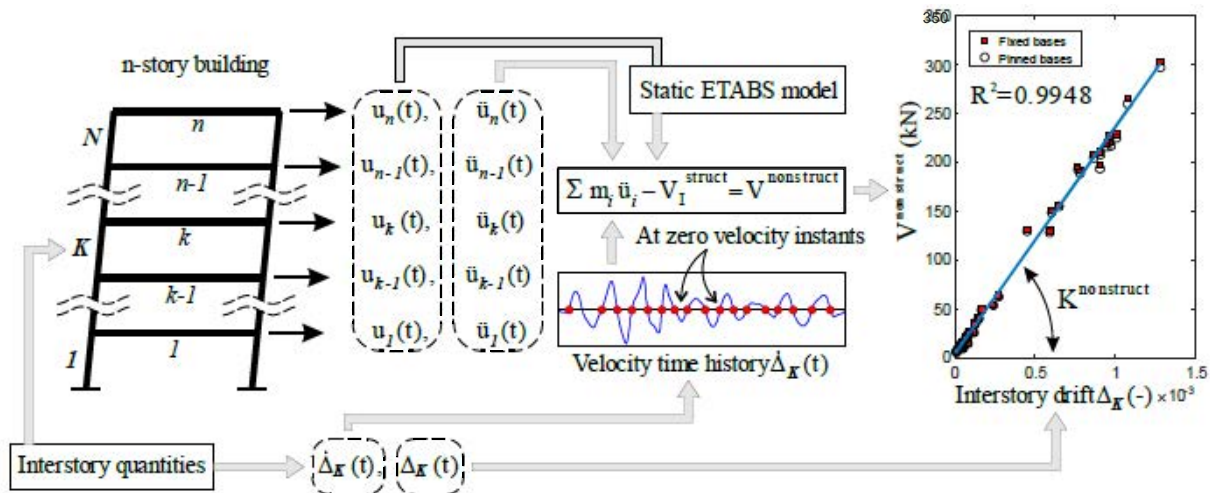
Figure 3. Process used for estimation of nonstructural stiffness.

Estimation of Nonstructural Stiffness

Nonstructural components (i.e., partition walls, cladding) contribute significantly (up to 40%) to the elastic stiffness of the building (NIST GCR 917 44 [15]), significantly affecting dynamic response. Thus, accurate characterization of nonstructural component stiffness is

essential for effective simulation of building response. The nonstructural stiffness within each story of the building may be estimated based on configuration of partition/external walls and cladding, based on test data (e.g., McMullin and Merrick [16]) and stiffness models (e.g., Kanvinde and Deierlein [17]) for similar types of nonstructural components. The stiffness of nonstructural wall and cladding details is sensitive to their geometry, the presence of doorways, captive ends, as well as construction details, e.g., type of studs (cold formed or wood), nail/screw patterns, sill plates (Kanvinde and Deierlein [17]; Jampole et al. [18]). As a result, literature-based estimates of nonstructural stiffness are approximate at best. Consequently, a direct approach for estimation of nonstructural stiffness was developed in this study, whose components are schematically illustrated in Figure 3.

Referring to this figure, this approach is based on the following observations and assumptions:

- During any ground motion, the instantaneous horizontal components of the story shear may be represented as $V_I^{story}{}_{x,y}(t)$ in which the subscript (Roman) I represents the Ith story, located directly below the ith floor (see Figure 3). The subscripts x and y represent the two horizontal directions.
- This instantaneous story shear may be decomposed into into three components, which must equilibrate the inertial forces of all the floors above story I:

$$V_I^{story}{}_{x,y}(t) = V_I^{NS}{}_{x,y}(t) + V_I^{struct}{}_{x,y}(t) + C_I^{damping}{}_{x,y} \cdot \dot{u}_{I,x,y}(t) = \sum_{i=I}^{N} m_i \cdot \ddot{u}_{i,x,y}(t) \qquad (1)$$

In the above equation, the terms $V_I^{NS}{}_{x,y}(t)$ and $V_I^{struct}{}_{x,y}(t)$ represent the instantaneous story shears (in the x and y directions) carried by the nonstructural and structural (i.e., SMRF and gravity frames) elements, respectively, whereas $C_I^{damping}{}_{x,y} \cdot \dot{u}_{x,y}(t)$ is the instantaneous damping force in which the term $\dot{u}_{x,y}(t)$ represents the instantaneous interstory velocities in the x and y directions. The term on the right hand side represents the inertial forces of all the floors above story I, in which $\ddot{u}_{i,x,y}(t)$ represents the instantaneous accelerations of these floors.

Following the observations above, the instantaneous force carried by the nonstructural elements $V_I^{NS}{}_{x,y}(t)$ may be determined if the remaining quantities in Equation 1 are estimated. To accomplish this, the following process is implemented for each building:

1. For a given story and direction within the building (e.g., the top story and x-direction), recorded time histories of interstory deformation (i.e., $u_{I,x,y}(t)$, interstory velocity $\dot{u}_{I,x,y}(t)$, and acceleration for all floors above the story (i.e., $\ddot{u}_{i,x,y}(t)$) are obtained. This process is conducted for multiple ground motions.
2. From these time histories, time instants at which the interstory velocity $\dot{u}_{I,x,y}(t)$, equals zero (or is negligible) are selected. At these instants, the damping force within the story is zero. Consequently, at each of these instants, the sum of the story shears carried by the structural frames and the nonstructural components must equal the inertial forces induced by stories above. This leads to the following equation:

$$V_I^{NS}{}_{x,y}(t) = \sum_{i=I}^{N} m_i \cdot \ddot{u}_{i,x,y}(t) - V_I^{struct}{}_{x,y}(t) \tag{2}$$

3. The term $V_I^{struct}{}_{x,y}(t)$ on the right-hand side denotes the shear force carried in the structural frames in story I. This shear force may be determined as follows. For the time instants selected above in Step 1, instantaneous values of the floor lateral displacements (i.e., $u_{I,x,y}(t)$) represent the deformations of the structural (i.e., SMRF and gravity frames) as well. Consequently, the story shear carried by these frames may be suitably estimated by applying these displacements in a static manner to the simulation model of the building (described earlier). In this context, it is important to note that the shear carried by the structural frames depends on lateral displacements as well as rotations of the joints at each story. For all joints except at the base, this may be addressed by allowing the joints to rotate freely following physical response (i.e., a statically condensed situation). However, the rotation of the base joint is not known; recall that examining base fixity is the main objective of this paper. This is problematic because from a theoretical standpoint, the base rotation influences the deformed shape of the entire structure, affecting the relationship between the story shears and the applied displacements. Nonetheless, from a practical standpoint only the story shears in the first story are sensitive to the base rotational flexibility. This is verified through a parametric study in which the base flexibility is varied from pinned to fixed, with the resulting variation in story shears being less than 5% (for all stories except for the first story). Given this observation the shears in the upper stories may be directly determined as $V_I^{struct}{}_{x,y}(t)$.

4. Once all the terms in Equation 2 are estimated as above, for each selected instant within each ground motion, the force in the nonstructural elements $V_I^{NS}{}_{x,y}(t)$ may be computed, and plotted against the corresponding interstory deformation $u_{I,x,y}(t)$ at that instant within the same ground motion. Figure 3 illustrates such a plot (for the top story of Building #1). The plot includes data from 8 ground motions, and a total of 60 data points, each corresponding to a time instant when velocity $\dot{u}_{I,x,y}(t)$ equals zero (or is negligible).

Referring to the scatter plot in Figure 3, two observations may be made: (1) a strong linear correlation is apparent between the interstory deformation $u_{I,x,y}(t)$ and the force carried by the nonstructural components, suggesting that the nonstructural elements may be appropriately represented as linear elastic elements within the building simulation, (2) the figure overlays data points from 8 ground motions – it is encouraging to note that the relationship has minimal variability between ground motions. These observations are consistent across all buildings and ground motions. Consequently, the nonstructural stiffness for each story within each building is determined through regression fitting of this data (in all cases, the R^2 value is not less than 0.98 indicating a strong linear trend). As an additional point of reference, the nonstructural stiffnesses determined in this study are similar to those for similarly sized buildings as reported in literature (Davies et al. [19]). Once determined in this way, the nonstructural stiffness is applied in the form of equivalent bracing members (see Figure 2, third column). These bracing members (whose cumulative stiffness equals the estimated story nonstructural stiffness) are inserted into bays where nonstructural elements (e.g., partition walls) are present. The process outlined in this section maximizes the accuracy of the building model itself, such that it may be used to

effectively interrogate the effect of column base flexibility. This is the subject of the next section.

Results and Discussion

Once the building models have been developed as described in the previous section, they are used to examine the effect of base fixity on seismic response. For this purpose, a parametric study is conducted; this includes the following:

1. For each of the buildings, column base connections are represented in five alternate ways. These include pinned (denoted k_0 to indicate zero fixity), fixed (denoted k_∞ to indicate infinite fixity) and three intermediate values. These values denoted k_{model}, $0.5k_{model}$, and $1.5k_{model}$ represent the model-based estimates of base fixity. Of these, the first k_{model} is the best-estimate of base fixity estimated using the appropriate model for each base detail within each building (referring to Table 1). Specifically, the model by Kanvinde et al. [10] is used to estimate the fixity of exposed base plate details (in Building #1), whereas the model by Torres-Rodas et al. [9] is used to estimate the fixity of embedded base connections (in Building #2). The estimates $0.5k_{model}$, and $1.5k_{model}$ (in which the base fixity is set to ±50% of the best estimate) are also queried to examine the sensitivity of frame response to uncertainty in base fixity estimates. Zero-length rotational springs with properties corresponding to each of these stiffness estimates are provided at the column bases. Two such springs are provided at each base, to represent the flexibility in either direction; these springs are calibrated to reflect the dimensions/anchor rod placement in each direction. Interaction between the two directions is not simulated.

2. The parametrization outlined above results in 10 building simulation models; five of these models (with k_0, k_∞, k_{model}, $0.5k_{model}$, and $1.5k_{model}$) correspond to each of the two buildings. All 10 models are subjected to all ground motions (see Table 1) available for the corresponding building.

3. Each of the 75 NLTHA runs (obtained from two buildings) produces acceleration time histories (at each story and in both directions) that may be directly compared to recordings from the instrumented buildings. Depending on the number of stories and density of instrumentation (e.g., not all stories are instrumented in all buildings), each of the buildings has a different number of acceleration time histories. As an illustrative example, Figure 4 shows graphical comparisons of recorded and simulated acceleration histories for Building #1.
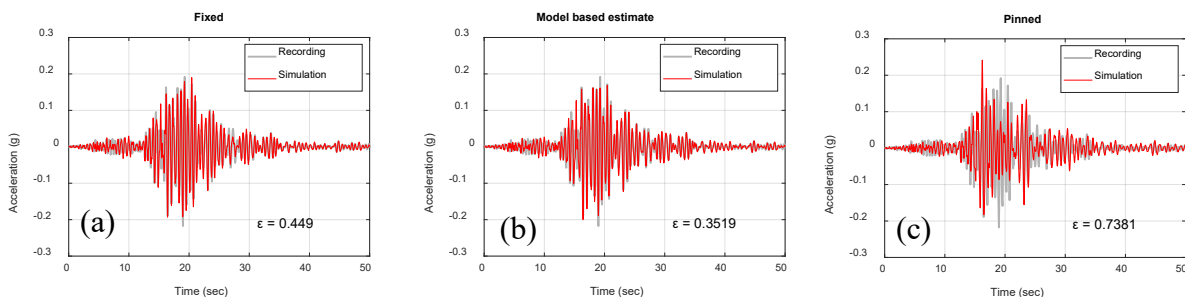
Figure 4. Sample recorded and simulated acceleration time histories for Building #1.

Each column overlays the simulated acceleration history corresponding to one representation of base fixity. Specifically, the recorded time histories in Figures 4a-c are identical, and correspond to the an accelerometer on the 3rd floor in the NS direction, whereas the simulated histories in each are different, corresponding to the k_0, k_{model}, and k_∞ base fixities. Significant torsional response was not noted in any of the buildings, such that the peak torsional rotation (in all cases/ground motions) was less than 2×10^{-4} rad.

Referring to Figure 4, it is observed that simulations with the fixed base k_∞ and the model based best-estimate k_{model} cases appear to track the recorded most closely, whereas simulations with the pinned base, i.e., k_0 show greater error. Although such visual assessment are informative, an objective error measure is needed to quantify agreement between simulated and recorded time histories, and to examine trends across various buildings or base details, and inform modeling practices in general. Naeim et al. [11] provide best practices for such quantification, in the specific context of utilizing CSMIP data; consequently, these practices are selected for this study. Specifically, the error between any pair of recorded and simulated time histories may be expressed as follows:

$$\varepsilon_{i,x,y} = \sum_{j=1}^{k} \frac{\int \left| \ddot{u}_{i,x,y,recorded} - \ddot{u}_{i,x,y,simulated} \right| \cdot dt}{\int \left| \ddot{u}_{i,x,y,recorded} \right| \cdot dt} \tag{3}$$

In the above equation, $\ddot{u}_{i,x,y,recorded}$ and $\ddot{u}_{i,x,y,simulated}$ refer to the recorded and simulated accelerations, respectively, at the ith story (in two orthogonal directions, i.e. N-S and E-W) at a given time instant j, whereas dt represents the time step. The error $\varepsilon_{i,x,y}$ is determined numerically. The error $\varepsilon_{i,x,y}$ calculated in this manner for the recorded and simulated time history pairs in Figures 4a-c is also shown on the corresponding figures. This provides a visual interpretation of the numerical value of the error as defined by Equation 3. The error measure $\varepsilon_{i,x,y}$ defined as above, is computed for all acceleration time history pairs arising from the 75 simulations and 15 recordings (obtained from two buildings). Figures 5a-b plot this error for all buildings versus the five levels of base fixity. Each of these figures contains two graphs. One represents the error (calculated as per Equation 3 above) from the acceleration time histories averaged over all instruments within the building – see graph denoted e_{total}. The second graph, denoted $e_{10\%}$ represents the error calculated by considering only the strong motion portion of each time history. Specifically, Equation 3 above is applied to all the time histories for only those values of acceleration that exceed 10% of the maximum acceleration within a time history. This provides a possibly more refined estimate, by discounting the error accumulated over low accelerations.
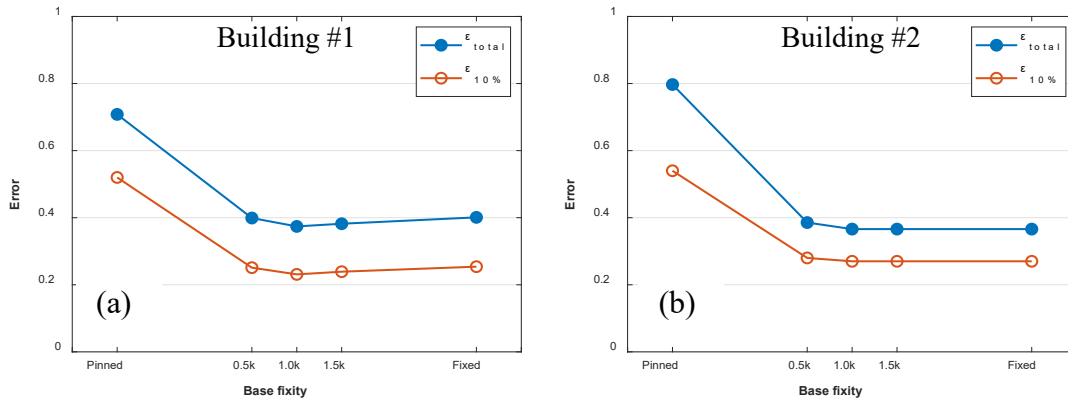
Figure 5. Error between simulated and recorded acceleration time histories.

Referring to Figures 5a-b, the following observations may be made:

- The pinned base assumption results in the greatest value of error. This suggests that simulating bases as pinned is grossly inaccurate. In fact, this error is quite large, i.e., both e_{total} and $e_{10\%}$ are greater than 0.5 even for Building #1 which includes only exposed type base connections. This suggests that the practice of simulating exposed base connection as pinned is not well-founded, and that the connection has significant rotational fixity, which is possibly enhanced by various factors including the presence of axial force as well as the overtopping slab.

- For Building #1 (i.e., Figure 5a), which features exposed base plate connections, the lowest error corresponds to k_{model}, such that the error increases as the fixity is increased beyond this value. Specifically, the simulations with k_{∞} result in roughly 2.5% more error (for both e_{total} and $e_{10\%}$) as compared to the simulations with k_{model}. This is unsurprising, given the higher flexibility of exposed base plate connections and suggests that for these connections, simulating the bases with model-based estimates of stiffness is appropriate.

- For Building #2 (i.e., Figure 5b), the errors (both e_{total} and $e_{10\%}$) decrease substantially as the base fixity is increased, and saturate around the fixity corresponding to k_{model} – such that increasing the stiffness to infinity (i.e., a fixed base) results in essentially the same response. Referring to Table 1, Building #2 has embedded base connections. This suggests that embedded base connections may be suitably represented either based on the appropriate model (i.e., Torres-Rodas et al. [9]) or even as fixed, especially since the former requires more effort and familiarity with the model.

- The lowest errors for Building #1 with the exposed bases are in the range of e_{total} 0.374, and $e_{10\%}$ 0.231; these are obtained using k_{model}. The lowest errors obtained for Building #2 with the embedded bases are e_{total} 0.366, and $e_{10\%}$ 0.27; as noted above, these are obtained for base stiffness between k_{model} and k_{∞}. In absolute terms these errors may be considered low/acceptable, considering the following: (1) Previous work, e.g., Naeim et al. [11] used genetic algorithms to tune building properties to minimize errors between CSMIP recordings and simulations – these algorithms resulted in errors (defined similarly) not significantly lower than the ones reported in Figures 5a-b. The simulations in this study were not optimized in this manner, and used best estimates of structural

properties, to provide a realistic assessment of expected errors in building simulation. From this standpoint, the error values noted above are encouraging, and (2) Referring to Figure 4b, the error corresponding to values in this range represents good visual agreement between the recordings and simulations.

- In all cases, the sensitivity of error to the base flexibility in the neighborhood of k_{model} is modest (as illustrated by the errors for the $0.5k_{model}$, and $1.5k_{model}$ simulations).
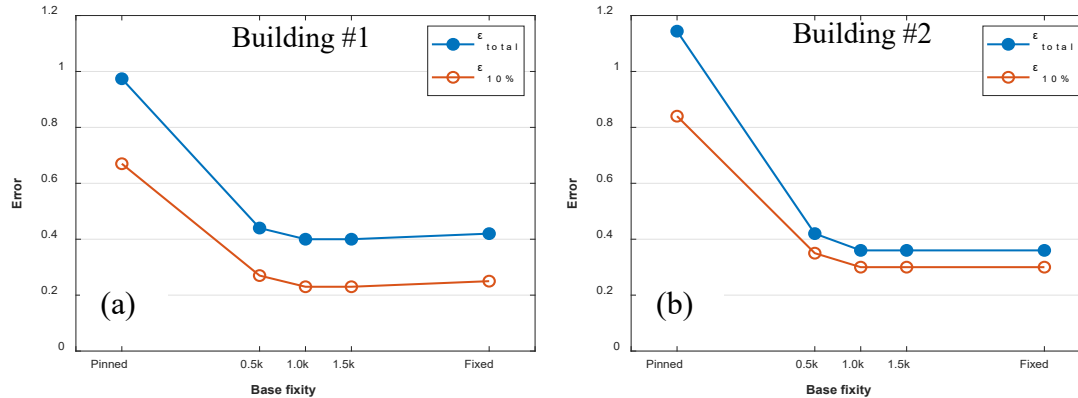
Figure 6. Error between simulated and recorded displacement time histories.

Figures 6a-b are similar to Figures 6a-b, except that they indicate errors for the recorded displacement time histories at each sensor. Such displacement time histories are provided by CSMIP and are based on integration as of the acceleration time histories as well as baseline corrections (Naeim et al. [11]). Both qualitatively and quantitatively, errors as well as the trends with respect to base fixity are similar between the acceleration and displacement time histories. This is not surprising, since the displacement time histories are derived from the acceleration time histories, but is informative nonetheless, since design and performance assessment require estimation of both the displacement as well as acceleration.

The observations from Figures 5-6 and associated discussion may be interpreted to provide guidance for the modeling of column base connections in steel moment frames. The key takeaways are:

- Simulating column bases as pinned, even when they are constructed as exposed base plates results in gross mischaracterization of frame response
- For exposed base plate connections, simulating the bases using model-based estimates is advisable, since it results in the best agreement (minimum errors) between the recorded and simulated time histories for both acceleration and displacement.
- For embedded base connections, simulating the bases as fixed or with the model based estimates result in the lowest error. This suggests that from a standpoint of elastic building response estimation, it is reasonable to simulate the bases as fixed, given the higher effort and expertise required for model-based estimation.
- Since the response appears to be relatively insensitive to the flexibility in a ±50% neighborhood of the model based estimates, explicit consideration of soil or footing flexibility may not be critical, since previous studies (Zareian and Kanvinde [4]) indicate that these effects do not alter the stiffness by more than 50%.

Summary and Conclusions

This paper uses earthquake recordings from the instrumented buildings to examine the efficacy of various assumptions and practices for modeling column base connections in steel moment frame buildings. Two moment frame buildings instrumented as part of the California Strong Motion Instrumentation Program (CSMIP) were selected for this study. The first building featured exposed base plate type connections, whereas the second one featured embedded column base connections. The methodology of the research involved constructing accurate simulation models for the superstructure, and then trialing a range of base flexibilities with this superstructure to examine the effect on agreement between the simulated and recorded time histories. To this end, simulation models were constructed for each of these buildings using the software ETABS; these models included numerous aspects of response, including geometric nonlinearity, finite joint size, and the simulation of all gravity frames. A sophisticated process was devised to estimate the stiffness associated with the nonstructural components. Each of these models was fitted with base rotational springs reflecting five alternate estimates of base fixity, ranging from pinned to fixed with intermediate values corresponding to model-based estimates. For each of these, the acceleration time histories resulting from the simulations were compared to their recorded counterparts. The agreement between these time history pairs (an indicator of the efficacy of the selected base flexibility) was quantified through an integrated error measure. This dependence of this error measure on numerous factors, pertaining to building/base configuration is studied with the objective of providing guidance regarding appropriate practices for simulating base connections.

The main findings include the following: (1) modeling the bases as pinned results in high error and is not recommended, even when the connection is of an exposed base plate type, (2) simulating bases with the appropriate model-based stiffness estimate (depending on whether they are embedded or exposed) generally results in low error (3) notwithstanding the previous point, in the case of embedded bases, modeling the bases as fixed provides a reasonably good agreement with recorded data and (4) the response is not highly sensitive to the estimated base flexibility, in the neighborhood of the model-based estimate.

Although this study provides the first field-recording based examination of column base fixity, it has limitations, which must be considered while interpreting or applying its recommendations. First, it is important to note that even the best overall agreement between simulated and recorded time histories is not ideal (errors on the order of 30% for the integrated measure), indicating that the representation of the base connections is only one source of error. Nonetheless, the lowest errors noted in this study are comparable to or better than those noted in other comparisons between recorded and high-fidelity simulations. The implications are the following: (1) although the remaining error may be reduced further by making some adjustments to the structural models, e.g., providing irregular strength, stiffness or damping values over various parts of the building, such adjustments are arbitrary with respect to the nominal or best-estimates of these properties, (2) as a result, the remaining error is challenging to minimize further, since it may be attributed to inherent uncertainty in these properties, and (3) the recommendations for simulating base fixity presented herein are justifiable within this overall context. Second, for the buildings studied in this paper, the ground motions were of relatively low intensity, selected to not induce inelastic actions in the structure. This has two additional

implications. First, the rotational response of base connections is nonlinear even in the pre-yield stage. This may be attributed to the following factors: (1) the nonlinearity of concrete, (2) gapping and contact between the steel and concrete components of the connection, and (3) for exposed base plate connections, the change in axial load during seismic loading, which results in a change in stiffness. This must be considered in extrapolating results of this study to buildings subjected to stronger shaking. Second, the results of this study indicate that the error between recorded and simulated time histories does not vary significantly for base fixities between k_{model} and k_∞. This appears to contradict previous findings by Zareian and Kanvinde [4] that indicate higher sensitivity of building response to base fixity. To explain this, it is noted that the Zareian and Kanvinde [4] examine inelastic collapse response of SMRFs. This response is controlled by soft-story formation, which in turn is greatly sensitive to base fixity. Thus, while the Zareian and Kanvinde [4] study underscores the importance of simulating base fixity, a similar degree of sensitivity is not observed in this study, whose objective is to provide insights regarding base flexibility using elastic simulations, rather than to simulate inelastic building response under stronger motions. Notwithstanding these limitations, the analyses presented in this paper are encouraging because they provide the first field-recording based guidance for simulating column base connections in Steel Moment Frames.

Acknowledgments

References

[1] American Institute of Steel Construction, Inc. (AISC). Seismic Provisions for Structural Steel Buildings (ANSI/AISC 341-16). Chicago, (IL, USA): American Institute of Steel Construction; 2016.
[2] American Institute of Steel Construction, Inc. (AISC). Prequalified Connections for Special and Intermediate Steel Moment Frames for Seismic Applications (ANSI/AISC 358-16). Chicago, (IL, USA): American Institute of Steel Construction; 2016.
[3] Fisher JM, Kloiber LA. Base Plate and Anchor Rod Design. AISC Steel Design Guide One, 2nd ed, American Institute of Steel Construction, Chicago, IL. 2006.
[4] Zareian F, and Kanvinde AM. Effect of Column-Base Flexibility on the Seismic Safety of Steel Moment-Resisting Frames. Earthquake Spectra, 29(4): 1537-1559, November 2013.
[5] Gomez IR, Kanvinde AM, Deierlein GG. Exposed Column Base Connections Subjected to Axial Compression and Flexure. Final Report Presented to the American Institute of Steel Construction, Chicago, IL. 2010.
[6] Barnwell N. Experimental Testing of Shallow Embedded Connections Between Steel

Columns and Concrete Footings. Master Thesis, Brigham Young University, Provo, UT. 2015.

[7] Grilli DA, Jones R, Kanvinde AM. Seismic Performance of Embedded Column Base Connections Subjected to Axial and Lateral Loads" Journal of Structural Engineering, ASCE. 143(5): 04017010, 2017.

[8] Tryon JE. Simple Models for Estimating the Rotational Stiffness of Steel Column to Footing Connections. Master Thesis, Brigham Young University, Provo, UT. 2016.

[9] Torres-Rodas P, Zareian F, Kanvinde AM. Rotational Stiffness of Deeply Embedded Column-Base Connections. Journal of Structural Engineering, ASCE, 143(8), August 2017.

[10] Kanvinde AM, Grilli DA, Zareian F. Rotational Stiffness of Exposed Column Base Connections: Experiments and Analytical Models. Journal of Structural Engineering, ASCE, 138(5): 549-560, May 2012.

[11] Naeim F, Hagie S, Alimoradi A, Miranda E. Automated Post-Earthquake Damage Assessment and Safety Evaluation of Instrumented Buildings. John A Martin and Associates Research Report – JAMA Report Number 2005-10639, Los Angeles, CA. 2005.

[12] Occupational Safety and Health Administration (OSHA), Safety Standards for Steel Erection, (Subpart R of 29 CFR Part 1926), Washington, D.C. 2001.

[13] Trautner CA, Hutchinson T, Grosser PR, Silva JF, Effects of Detailing on the Cyclic Behavior of Steel Baseplate Connections Designed to Promote Anchor Yielding. Journal of Structural Engineering, ASCE, 142(2), February 2016.

[14] Computers and Structures, Inc. (CSI). ETABS Integrated Building Design Software. (http://docs.csiamerica.com/manuals/etabs/Analysis%20Reference.pdf), Computers and Structures Inc., Berkeley, CA, 2016.

[15] ATC, Seismic Analysis, Design, and Installation of Nonstructural Components and Systems – Background and Recommendations for Future Work, Report No. NIST GCR 17-917-44, Applied Technology Council, Redwood City, CA, 2017.

[16] McMullin K, Merrick D. Seismic Performance of Gypsum Walls - Experimental Test Program, Report W-15, CUREE Woodframe Project, 2001.

[17] Kanvinde AM, Deierlein GG. Analytical Models for the Seismic Performance of Gypsum Drywall Partitions. Earthquake Spectra, 22(2): 391-411, May 2006.

[18] Jampole E, Deierlein GG, Miranda E, Fell B, Swensen S, Acevedo C. Full-Scale Dynamic Testing of a Sliding Seismically Isolated Unibody House. Earthquake Spectra, 32(4): 2245-2270, November 2016.

[19] Davies R, Retamales R, Mosqueda G, Filiatrault A, Allen D. Effects of Cold-formed Steel Framed Gypsum Partition Walls on the Seismic Response of a Medical Facility. Twenty-First International Specialty Conference on Cold-Formed Steel Structures, St. Louis, Missouri. 2012.